

## Spin Transitions in a Dithiazolyl Radical: Preparation, Crystal Structures, and Magnetic Properties of 3-Cyanobenzo-1,3,2-dithiazolyl, $C_7H_3S_2N_2\cdot$

Antonio Alberola, Rebecca J. Collis, Simon M. Humphrey, Robert J. Less, and Jeremy M. Rawson\*

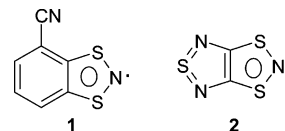
Department of Chemistry, The University of Cambridge, Lensfield Road, Cambridge CB2 1EW, U.K.

Received November 9, 2005

The incorporation of the electronegative cyano group into the structure of the title dithiazolyl radical **1** induces a lamellar packing motif that favors spin-transition behavior. Variable-temperature magnetic studies on **1** reveal a reversible phase transition at 250 K between a diamagnetic low-temperature phase and a paramagnetic high-temperature phase. X-ray crystal structures at 180(2) and 300(2) K reveal that both phases crystallize in the space group  $P2_1/c$ , with the phase transition associated with a doubling of the crystallographic  $a$  axis. The concomitant change in magnetic properties is associated with a change from a paramagnetic regular  $\pi$  stack of radicals and a diamagnetic distorted  $\pi$  stack in which an energy gap opens up at the Fermi level corresponding to a Peierls-like transition.

Dithiazolyl radicals constitute one member of a family of thermally stable sulfur–nitrogen  $\pi$  radicals whose properties have been investigated extensively as building blocks for the construction of both conducting and magnetic materials.<sup>1</sup> A number of these dithiazolyl radicals have previously been reported to exhibit phase transitions between an enthalpically stabilized diamagnetic  $\pi^*-\pi^*$  dimer and an entropically favored paramagnetic radical.<sup>2</sup> In each case, the phase transition has been associated with some region of bistability, i.e., a temperature range in which both low- and high-temperature phases can coexist. The resultant physical properties in this region are then dependent on the sample history. Awaga and co-workers have shown<sup>3</sup> that the

transition between the two phases of the trithiazapentalenyl radical (**2**) can be driven both thermally and photochemically in a manner reminiscent of spin-crossover transitions in transition-metal complexes. The latter have already been identified as potential “smart” materials with potential applications in data storage and photoswitchable materials inter alia.<sup>4</sup> For transition-metal complexes, the spin transition is manifested in changes in the bond lengths to the metal.<sup>4</sup> As a result of flexibility in the ligand framework, there is frequently a lack of cooperativity, and these spin transitions often occur without hysteresis. In the case of dithiazolyl radicals, the electronic changes are linked to a change in the packing from a diamagnetic dimeric  $\pi$ -stacked arrangement (with intra- and interdimer  $S\cdots S$  distances of ca. 3.2 and 3.8 Å, respectively) to a regularly spaced paramagnetic monomeric  $\pi$  stack (with inter-radical separations of ca. 3.6 Å). The thermal hysteresis in these systems can often be extremely large, e.g., ca. 90 K in **2**. Elegant structural studies by Oakley have identified several cooperative mechanisms for the solid–solid-phase transitions in a number of these dithiazolyl derivatives.<sup>5</sup> The activation energy to interconversion, which lies at the origin of the bistability, has been proposed to arise through the cooperative breaking of intermolecular interstack  $S\cdots N$  contacts, which are of a predominantly electrostatic nature.<sup>5</sup> We now report the solid-state structures and magnetic properties of the first dithiazolyl radical (**1**) to exhibit a spin transition without



thermal hysteresis. A comparison of the high- and low-temperature structures reveals that the phase transition can occur without cleavage of the intermolecular contacts.

\* To whom correspondence should be addressed. E-mail: jmr31@cus.cam.ac.uk.

- (1) (a) Cordes, A. W.; Haddon, R. C.; Oakley, R. T. *Adv. Mater.* **1994**, *10*, 798. (b) Rawson, J. M.; Palacio, F. *Struct. Bonding* **2001**, *100*, 93.  
 (2) (a) Barclay, T. M.; Cordes, A. W.; deLaat, R. H.; Goddard, J. D.; Haddon, R. C.; Jeter, D. Y.; Mawhinney, R. C.; Oakley, R. T.; Palstra, T. T. M.; Patenaude, G. W.; Reed, R. W.; Westwood, N. P. C. *J. Am. Chem. Soc.* **1997**, *119*, 2633. (b) Fujita, W.; Awaga, K. *Science* **1999**, *286*, 281. (c) McManus, G. D.; Rawson, J. M.; Feeder, N.; McInnes, E. J. L.; Novoa, J. J.; Burriel, R.; Palacio, F.; Olliete, P. *J. Mater. Chem.* **2001**, *11*, 1992. (d) Brusso, J. L.; Clements, O. P.; Haddon, R. C.; Itkis, M. E.; Leitch, A. A.; Oakley, R. T.; Reed, R. W.; Richardson, J. F. *J. Am. Chem. Soc.* **2004**, *126*, 8256. See also refs 5 and 6.

- (3) Matsuzaki, H.; Fujita, W.; Awaga, K.; Okamoto, H. *Phys. Rev. Lett.* **2003**, *017403*.

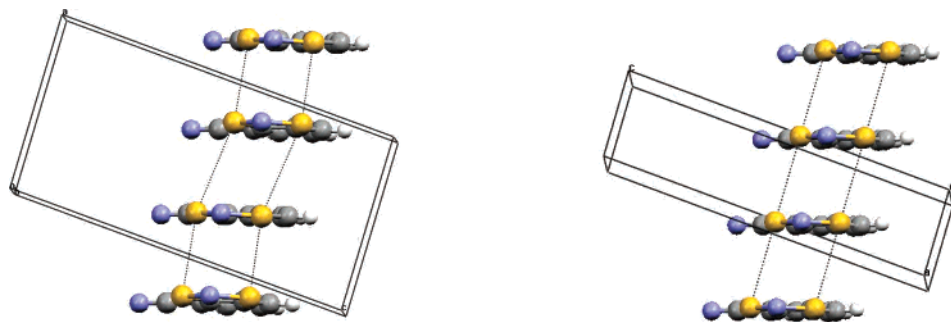
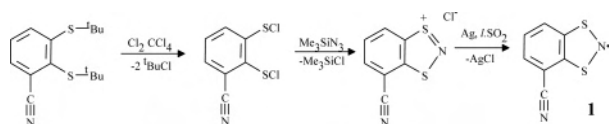


**Figure 1.** X-ray structures of **1** viewed perpendicularly to the crystallographic *a* axis: (left) at 180(2) K; (right) 300(2) K.

### Scheme 1



While dithiazolyl radicals adopt a variety of packing motifs, only those with a  $\pi$ -stacked, lamellar structure have been shown to exhibit bistability. This motif is promoted by the presence of electrostatically favorable  $S^{\delta+}\cdots N^{\delta-}$  in-plane interactions between the dithiazolyl S atom and N atoms of either the dithiazolyl ring<sup>4</sup> or a heterocyclic substituent.<sup>6,7</sup> To prepare new planar,  $\pi$ -stacked derivatives that might specifically exhibit this type of behavior, we targeted the cyano-functionalized benzodithiazolyl radical **1**. Previous studies on dithiadiazolyl radicals have shown a strong tendency to form in-plane  $CN\cdots S$  contacts,<sup>8</sup> while “side-on”  $CN\cdots NC$  contacts have also been observed in benzonitrile derivatives.<sup>8f</sup>

Radical **1** was prepared via a modification of the literature method in which the key sulfenyl chloride intermediate was prepared by direct chlorination of bis(*tert*-butylthio)benzotrile (Scheme 1). Chlorination of  $C_6H_3(CN)(S^tBu)_2$  (1 g, 3.5 mmol) in  $CCl_4$  (20 mL) under ambient conditions yielded an orange solution of  $C_6H_3(CN)(S^tBu)_2$ . The solvent was removed in vacuo and the oily residue redissolved in  $CH_2Cl_2$ . This was treated with  $Me_3SiN_3$  (0.4 mL, 5 mmol) to yield the salt  $[C_6H_3(CN)S_2N]^+Cl^-$ , [**1**]Cl. Reduction of [**1**]Cl with Ag powder in  $SO_2$  yielded **1**, which was purified by

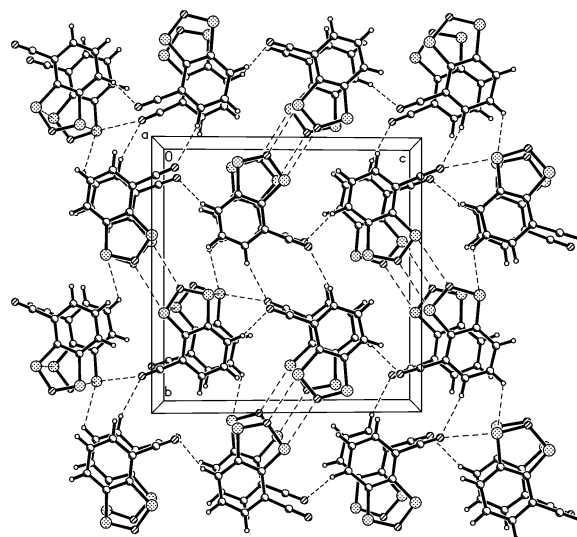


**Figure 2.** Projection of the X-ray structure of **1** at 180(2) K in the *bc* plane.

vacuum sublimation, affording dark-red blocks. [Yield: 0.236 g, 35%. Anal. Found (calcd for  $C_7H_3S_2N_2$ ): C, 46.4 (46.9); H, 1.9 (1.7); N, 15.3 (15.6). MS (EI<sup>+</sup>): *m/z* (%) 179 (73,  $C_7H_3N_2S_2$ ), 165 (32,  $C_7H_3S_2N$ ).] The X-band electron paramagnetic resonance was recorded on a sample dissolved in toluene. A characteristic triplet was observed with  $g = 2.0061$  and  $a_N = 11.1$  G.] The crude product was purified and crystallized by vacuum sublimation at 70–35 °C at  $10^{-1}$  Torr. The crystal structure of **1** at 180(2) K revealed a dimeric structure, with two molecules in the asymmetric unit forming a cisoid dimer similar to that seen in a number of other derivatives.<sup>9</sup> The intradimer  $S\cdots S$  contacts are 3.263 and 3.347 Å.

These dimers are linked along the crystallographic *a* axis by longer  $S\cdots S$  contacts (3.886 and 3.971 Å), generating a distorted  $\pi$ -stacked structure (Figure 1a). In the *bc* plane, dimers are linked via heterocyclic  $S\cdots N$  contacts (3.149 and 3.287 Å; Figure 2) comparable to the sum of the in-plane van der Waals radii (3.2 Å).<sup>10</sup> The cyano group forms  $CN\cdots S$  contacts (3.598 and 3.621 Å), but these fall well beyond the sum of the van der Waals radii. Conversely, two

(4) Gütllich, P.; Rovira, C.; Goodwin, H. A. *Chem. Soc. Rev.* **2000**, 29, 419. See also *Top. Curr. Chem.* **2004**, 233 and 234, dedicated to this topic.

(5) Brusso, J. L.; Clements, O. P.; Haddon, R. C.; Itkis, M. E.; Leitch, A. A.; Oakley, R. T.; Reed, R. W.; Richardson, J. F. *J. Am. Chem. Soc.* **2004**, 126, 14692.

(6) Barclay, T. M.; Cordes, A. W.; George, N. A.; Haddon, R. C.; Oakley, R. T.; Palstra, T. T. M.; Patenaude, G. W.; Reed, W.; Richardson, J. F.; Zang, H. J. *Chem. Soc., Chem. Commun.* **1997**, 873.

(7) Barclay, T. M.; Cordes, A. W.; George, N. A.; Haddon, R. C.; Itkis, M. E.; Mashuta, M. S.; Oakley, R. T.; Patenaude, G. W.; Reed, W.; Richardson, J. F.; Zang, H. J. *Am. Chem. Soc.* **1998**, 120, 352.

(8) (a) Cordes, A. W.; Haddon, R.; Hicks, R. G.; Oakley, R. T.; Palstra, T. T. M. *Inorg. Chem.* **1992**, 31, 1802. (b) Banister, A. J.; Bricklebank, N.; Clegg, W.; Elsegood, M. R. J.; Gregory, C. I.; Lavender, I.; Rawson, J. M.; Tanner, B. K. *Chem. Commun.* **1995**, 679. (c) Banister, A. J.; Bricklebank, N.; Lavender, I.; Rawson, J. M.; Gregory, C. I.; Tanner, B. K.; Clegg, W.; Elsegood, M. R. J.; Palacio, F. *Angew. Chem., Int. Ed. Engl.* **1996**, 35, 2533. (d) Antorrena, G.; Brownridge, S.; Cameron, T. S.; Palacio, F.; Parsons, S.; Passmore, J.; Thompson, L. K.; Zarlaida, F. *Can. J. Chem.* **2002**, 80, 1568. (e) Cordes, A. W.; Chamchoumis, C. M.; Hicks, R. G.; Oakley, R. T.; Young, K. M.; Haddon, R. C. *Can. J. Chem.* **1992**, 70, 9. (f) Alberola, A.; Less, R. J.; Palacio, F.; Pask, C. M.; Rawson, J. M. *Molecules* **2004**, 9, 771.

(9) (a) Brownridge, S.; Du, H.; Fairhurst, S. A.; Haddon, R. C.; Oberhammer, H.; Parsons, S.; Passmore, J.; Schriver, M. J.; Sutcliffe, L. H.; Westwood, N. C. P. *J. Chem. Soc., Dalton Trans.* **2000**, 3365. (b) Wolmershauser, G.; Kraft, G. *Chem. Ber.* **1990**, 123, 881.

(10) Nyburg, S. C.; Faerman, C. H. *Acta Crystallogr., Sect. B* **1985**, 41, 274.

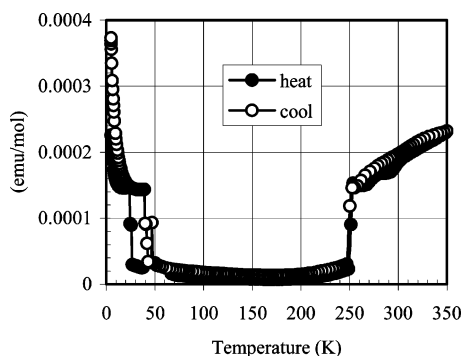


**Figure 3.** Temperature dependence of  $\chi$  upon cooling and heating of **1** between 2 and 350 K.

cyano groups are displaced in an antiparallel fashion about an approximate inversion center. While the contacts between cyano groups (3.851–3.901 Å) are longer than similar contacts reported previously,<sup>11</sup> they are similar to those supported by lateral interactions to the aromatic protons (C–H···N in the range of 2.520–2.645 Å).<sup>12</sup>

The structure of **1** recorded at 300(2) K falls in the same space group ( $P2_1/c$ ) but with a halving of the crystallographic  $a$  axis and a single molecule in the asymmetric unit. It exhibits a packing motif in the  $bc$  plane similar to that of the 180 K structure, with comparable heterocyclic S···N (3.322 Å) and CN···S (3.556 Å) contacts. However, the intermonomer contacts along the  $\pi$ -stacking direction (the crystallographic  $a$  axis) are now all equivalent and equal to the  $a$ -axis spacing (3.665 Å; Figure 1b). Unit cell determinations on a single crystal over the temperature range of 180–300 K indicate that the phase transition occurs between 245(2) and 255(2) K.

Magnetic susceptibility measurements on polycrystalline samples of **1** were made on a Quantum Design SQUID magnetometer in an applied field of 5000 G between 5 and 350 K. Data were corrected for both sample diamagnetism

(Pascal's constants) and the sample holder. The sample is diamagnetic between 50 and 250 K but undergoes an abrupt transition to a paramagnetic state upon warming above 250 K, in agreement with the observed structural transition. This transition is reversible (Figure 3) but shows no evidence of thermal hysteresis. Above 250 K, the value of  $\chi T$  increases steadily up to 350 K, reaching a value of 0.08 emu·K·mol<sup>-1</sup>, just 20% of that expected for an  $S = 1/2$  paramagnet. This is consistent with a strongly antiferromagnetically coupled regime and comparable to the value of 0.16 emu·K·mol<sup>-1</sup> at 350 K for the trithiaziazapentalenyl radical.<sup>2b,c</sup>

In the case of **1**, the phase transition appears to occur via a simple Peierls distortion along the  $a$  axis. The retention of the same space group symmetry means that the transformation does not require any disruption of the in-plane contacts and, as a consequence, the phase transition occurs without hysteresis.

Upon cooling below 50 K, the sample undergoes a second phase transition. In contrast to the transition at 250 K, this low-temperature transition does exhibit thermal hysteresis ( $T_{C1} = 39$  K and  $T_{C1} = 26$  K; Figure 3). The susceptibility in the low-temperature region corresponds to less than 2% of the sample exhibiting Curie–Weiss behavior. However, the discontinuity in  $\chi$  mitigates against simple contamination with an  $S = 1/2$  Curie spin, and the low-temperature paramagnetism of **1** does not obey either Curie- or Curie–Weiss-type behavior. Further studies are in progress to probe the structure of **1** below 40 K.

**Acknowledgment.** We thank the EPSRC for financial support (R.J.L., R.J.C., and S.M.H.) and Homerton College for a Research Fellowship (A.A.). The authors also thank J. M. Martinez-Agudo for his help with the SQUID measurements.

**Supporting Information Available:** Electrochemical studies on the salt [**1**]Cl and crystallographic files in CIF format. This material is available free of charge via the Internet at <http://pubs.acs.org>.

(11) Kubicki, M. *Acta Crystallogr., Sect. C* **2004**, *60*, 0225.

(12) da Silva, J. P.; Silva, M. R.; Ramos, M. N. *J. Braz. Chem. Soc.* **2005**, *16*, 844.

IC051935P